Nicotinamide N-Methyltransferase Expression Decreases in Iron Overload, Exacerbating Toxicity in Mouse Hepatocytes

Tiago Koppe,[1–3] Bonnie Patchen,[1–3] Aaron Cheng,[1–3] Manoj Bhasin,[3,4] Chris Vulpe,[5] Robert E. Schwartz,[6] Jose Maria Moreno-Navarrete,[7,8] Jose Manuel Fernandez-Real,[7,8] Pavlos Pissios,[9] and Paula G. Fraenkel[1–3]

Iron overload causes the generation of reactive oxygen species that can lead to lasting damage to the liver and other organs. The goal of this study was to identify genes that modify the toxicity of iron overload. We studied the effect of iron overload on the hepatic transcriptional and metabolomic profile in mouse models using a dietary model of iron overload and a genetic model, the hemojuvelin knockout mouse. We then evaluated the correlation of *nicotinamide N-methyltransferase (NNMT)* expression with body iron stores in human patients and the effect of *NNMT* knockdown on gene expression and viability in primary mouse hepatocytes. We found that iron overload induced significant changes in the expression of genes and metabolites involved in glucose and nicotinamide metabolism and that *NNMT*, an enzyme that methylates nicotinamide and regulates hepatic glucose and cholesterol metabolism, is one of the most strongly down-regulated genes in the liver in both genetic and dietary iron overload. We found that hepatic *NNMT* expression is inversely correlated with serum ferritin levels and serum transferrin saturation in patients who are obese, suggesting that body iron stores regulate human liver *NNMT* expression. Furthermore, we demonstrated that adenoviral knockdown of *NNMT* in primary mouse hepatocytes exacerbates iron-induced hepatocyte toxicity and increases expression of transcriptional markers of oxidative and endoplasmic reticulum stress, while overexpression of *NNMT* partially reversed these effects. *Conclusion*: Iron overload alters glucose and nicotinamide transcriptional and metabolic pathways in mouse hepatocytes and decreases *NNMT* expression, while *NNMT* deficiency worsens the toxic effect of iron overload. For these reasons, *NNMT* may be a drug target for the prevention of iron-induced hepatotoxicity. (*Hepatology Communications* 2017;1:803-815)

Introduction

Iron is a critical element in all mammals. It is required for the transport of oxygen throughout the body, for DNA synthesis, and for respiration. Because of its ability to catalyze the production of reactive oxygen species by way of the Fenton reaction,[(1)] iron excess causes tissue injury and even organ failure. As mammals have no active means of excreting iron, iron homeostasis is regulated by adjusting the amount of iron absorbed from the diet in the duodenum or released from storage in macrophages. This is accomplished by hepcidin, an iron regulatory peptide hormone that interacts with the iron exporter ferroportin (SLC40a1) to cause its internalization and degradation.[(2)] The liver is the major source of hepcidin; thus, the liver plays a critical role in sensing and responding to systemic iron overload. Iron sensing in the mouse or human liver occurs through increases in bone morphogenic protein (BMP) expression and activation of

Abbreviations: BMP, bone morphogenic protein; FABP, fatty acid binding protein; FAC, ferric ammonium citrate; FBS, fetal bovine serum; FDR, false discovery rate; FTH, ferritin heavy chain; HJV, hemojuvelin; LC-MS, liquid chromatography–mass spectrometry; LC-MS/MS, tandem liquid chromatography–mass spectrometry; MNAM, N1-methylnicotinamide; NAD+, nicotinamide adenine dinucleotide; NADH, reduced nicotinamide adenine dinucleotide; NADP, nicotinamide adenine dinucleotide phosphate; NAM, nicotinamide; NNMT, nicotinamide N-methyltransferase; PPAR, peroxisome proliferator activated-receptor; SAH, S-adenosyl homocysteine; SAM, S-adenosyl methionine; shRNA, short hairpin RNA; Smad, mothers against decapentaplegic; WT, wild type.

Received March 17, 2017; accepted August 1, 2017.
Additional Supporting Information may be found at onlinelibrary.wiley.com/doi/10.1002/hep4.1083/full.

mothers against decapentaplegic (Smad) signaling.[3-5] The BMP coreceptor hemojuvelin (HJV) interacts with BMP receptors on the hepatocyte membrane to potentiate Smad signaling and increase transcription of hepcidin. Deficiency in hepcidin or HJV is associated with iron overload both in human patients and in mouse models.[6-9]

As the prevalence of obesity is rising throughout the developed world and is associated with increased rates of diabetes, hyperlipidemia, and steatohepatitis, the interplay of energy metabolism and iron metabolism is an increasing area of interest.[10] Obesity has been associated with iron deficiency and an impaired response to oral iron supplementation in children and adolescents.[11-13] Although the mechanisms governing the effect of obesity on iron absorption are not completely understood, obesity has been associated with lower serum iron levels but higher serum levels of C-reactive protein, transferrin receptor, ferritin, hepcidin, leptin, and interleukin-6.[14-16] On the other hand, increased body iron stores are associated with an increased risk of diabetes mellitus[17] and alterations in hepatic glucose metabolism.[17]

Niacin, also known as vitamin B3, includes nicotinic acid and nicotinamide (NAM).[18] It is an essential vitamin that has been used for many years to reduce serum cholesterol levels.[19] NAM is a precursor for nicotinamide adenine dinucleotide (NAD+), the cofactor for numerous enzymes involved in the oxidation of energy sources and the conversion of carbohydrates to lipids.[18,20] The enzyme nicotinamide N-methyltransferase (NNMT) (Fig. 1A), alters NAM to N1-methylnicotinamide (MNAM) using the universal methyl donor S-adenosyl methionine (SAM). SAM is converted in the process to S-adenosyl homocysteine (SAH).[21,22] Recent studies have demonstrated that NNMT deficiency in adipocytes protects against diet-induced obesity by increasing energy

Supported by the National Institutes of Health (R01 DK085250 to P.G.F.; R01 GM083198 to C.V. and P.G.F.; DK083694 to P.P.; K08 DK101754 to R.E.S.), Conselho Nacional de Desenvolvimento Cientifico e Tecnologico, Brazil (to T.K.), the Harvard College Research Program (to A.C.), the Spanish Ministry of Health (FIS 2015-01934) and Centro de Investigación Biomédica en Red de Fisiopatología de la Obesidad y la Nutrición (an initiative of the Instituto de Salud Carlos III; to J.M.F.), and the Alice Bohmfalk Charitable Trust (to R.E.S.).

Funding sources played no role in the design of the research, writing of the report, or the decision to publish.

View this article online at wileyonlinelibrary.com.

DOI 10.1002/hep4.1083

Potential conflict of interest: Dr. Fraenkel currently receives salary support from Sanofi, but Sanofi did not fund or design this research and has no commercial interest in this project or responsibility for its content.

ARTICLE INFORMATION:

From the [1]Division of Hematology/Oncology and [2]Cancer Research Institute, Beth Israel Deaconess Medical Center, Boston, MA; [3]Department of Medicine, Harvard Medical School, Boston, MA; [4]Division of Interdisciplinary Medicine and Biotechnology, Beth Israel Deaconess Medical Center, Boston, MA; [5]Department of Physiological Sciences, University of Florida, Gainesville, FL; [6]Division of Gastroenterology and Hepatology, Weill Cornell Medical School, New York, NY; [7]Department of Diabetes, Endocrinology and Nutrition, Institut d'Investigació Biomèdica de Girona, Hospital de Girona Dr. Josep Trueta and Universitat de Girona, Girona, Spain; [8]CIBER Fisopatologia de la Obesidad y Nutricion, Instituto de Salud Carlos III, Madrid, Spain; [9]Division of Endocrinology, Beth Israel Deaconess Medical Center, Boston, MA.

ADDRESS CORRESPONDENCE AND REPRINT REQUESTS TO:

Paula G. Fraenkel, M.D.
Division of Hematology/Oncology
Beth Israel Deaconess Medical Center, CLS 428
330 Brookline Avenue
Boston, MA 02215
E-mail: pfraenkel@post.harvard.edu
Tel: + 1-857-998-1785
or

Pavlos Pissios, Ph.D.
Division of Endocrinology
Beth Israel Deaconess Medical Center, CLS 734
330 Brookline Avenue
Boston, MA 02215
Tel: + 1-617-735-3278
E-mail: ppissios@bidmc.harvard.edu

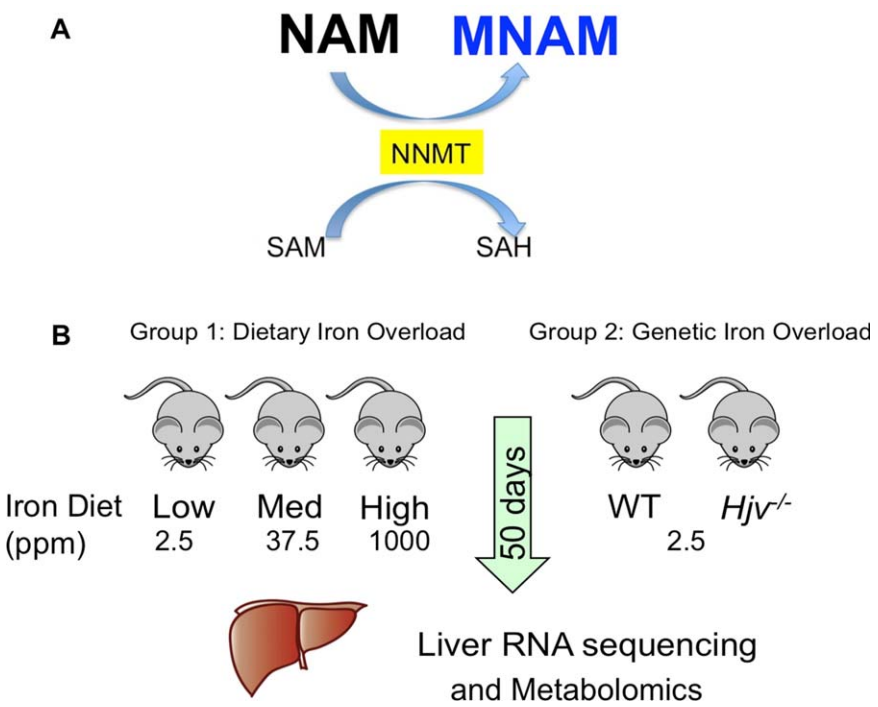

FIG. 1. Mouse models reveal the interactions of iron overload and cellular metabolism. (A) The function of NNMT. NNMT catalyzes the methylation of NAM to MNAM and converts the methyl donor SAM to SAH. (B) Dietary and genetic models of iron overload. For the dietary iron-overload model, 5-week-old WT C57BL6 male mice were placed on a soy-free diet (AIN-93G) that was iron deficient (2.5 mg/kg, n = 3), iron sufficient (37.5 mg/kg, n = 3), or high iron (1,000 mg/kg, n = 3). For the genetic iron-overload model, 5-week-old mice that were either WT or *HJV*$^{-/-}$ gene mice (n = 2 per group) were maintained on the iron-deficient diet (2.5 mg/kg iron). After 50 days, the mice were killed and RNA and polar metabolites were extracted for next-generation sequencing or LC-MS/MS analysis, respectively.

expenditure, while NNMT in hepatocytes regulates glucose, lipid, and cholesterol metabolism.[21,22]

In this report, we employed RNA sequencing and metabolomic approaches to identify the pathways affected by iron overload in mouse hepatocytes. We found that pathways regulating glucose and NAM metabolism were significantly altered in both a dietary model of iron overload and a genetic model, the *HJV* knockout mouse, and that *NNMT* was significantly down-regulated in both models. In a group of obese patients, we discovered that hepatic *NNMT* transcript levels inversely correlated with measures of body iron stores, including serum iron, serum ferritin, and serum transferrin saturation levels. Furthermore, we demonstrated that iron loading human or mouse hepatocytes *in vitro* suppressed *NNMT* expression. Adenoviral knockdown of *NNMT* expression in mouse hepatocytes enhanced iron-induced cytotoxicity and increased expression of genes responsive to oxidative or endoplasmic reticulum stress. Taken together, these findings indicate that hepatocyte iron overload suppresses *NNMT* transcript levels, which in turn exacerbates the toxic effects of iron.

Materials and Methods

MOUSE STRAINS, RNA PREPARATION, AND MEASUREMENT OF NONHEME IRON LEVELS

Ethical approval was obtained from the institutional animal care and use committee of Beth Israel Deaconess Medical Center (Animal Welfare Assurance #A3153-01; Boston, MA) in accord with national and international guidelines. All wild-type (WT) mice were C57BL6 males (Jackson Laboratory, Bar Harbor, ME). Professor Nancy Andrews (Jackson Laboratory) provided *HJV* knockout (*HJV*$^{-/-}$) mice on a C57BL6 background.[7] For the dietary study, at 5 weeks of age, the mice were transitioned to a soy-free diet (AIN-93G; Bioserv, Flemington, NJ) containing different amounts of iron per kilogram of food: iron deficient (2.5 mg/kg, n = 3), iron sufficient (37.5 mg/kg, n = 3), or iron excess (1,000 mg/kg, n = 3). For the genetic study, 5-week-old mice that were either WT or *HJV*$^{-/-}$ (n = 2 mice per group) were maintained on the iron-deficient diet. After 50 days, the mice were killed and

liver RNA was extracted using the RNeasy Mini Kit (Qiagen, Valencia, CA) according to the manufacturer's instructions. Hepatic nonheme iron stores were measured using the bathophenanthroline method as described.[23]

RNA SEQUENCING

One microgram of RNA from each sample was sequenced with a HiSeq 2000 (Illumina, Inc., San Diego, CA). Additional bioinformatics and analysis methods are provided in the Supporting Methods. Unsupervised analysis was performed on normalized and preprocessed count data using correlation-based hierarchical clustering and principal component analysis. The normalized count data were compared among groups in an unpaired manner using a negative binomial model to identify differentially expressed genes. The differentially expressed genes were identified on the basis of false discovery rate (FDR) and fold change. To identify the set of genes depicting a strong association with iron dose (i.e., low, iron sufficient, and high), the differential expression profiles from the different groups were further analyzed using self-organizing map clustering.[24] In the genetic iron-overload experiment, an FDR <0.05 and a mean fold change >2 were used to reveal genes that were differentially expressed compared to WT mice. All raw and processed RNA sequencing data can be found at http://www.ncbi.nlm.nih.gov/geo/ under accession numbers GSE86236 and GSE86292.

Pathway analysis was performed using DAVID Bioinformatics Resources 6.7.[25,26]

METABOLOMICS SAMPLE PREPARATION AND ANALYSIS

We extracted 5-10 mg mouse liver tissue in 80% high-performance liquid chromatography-grade methanol, as described, then lyophilized and resuspended the extract in 20 μL of liquid chromatography–mass spectrometry (LC-MS)-grade water. Next, 5-10 μL of each sample was autoinjected into the QTRAP 5500 tandem LC-MS (LC-MS/MS) system (AB Sciex, LLC, Framingham, MA). Multiquant 2.0 software (AB Sciex, LLC) was used to quantify chromatographic peak areas. The Linear Models for Microarray Analysis package[27] from the Bioconductor project was used to identify differentially expressed molecules among different groups compared to controls. Technical replicates were averaged, and the biologically distinct sample groups were compared by fitting a linear model for each variable (normalized expression values) and applying empirical Bayes smoothing to identify differentially expressed molecules. For pathway analysis, the differentially expressed molecules ($P \leq 0.05$ and fold change > 2) were grouped into pathways using Metaboanalyst 3.0.[28]

QUANTITATIVE REAL-TIME REVERSE-TRANSCRIPTION POLYMERASE CHAIN REACTION

We extracted RNA and generated complementary DNA according to the described method[29] to measure the transcript levels of *hepcidin, NNMT*, and other genes by quantitative real-time reverse-transcription polymerase chain reaction using primers and probes as described (Supporting Table S1 or available on request). Data shown are means ± SEM unless otherwise indicated. Student *t* tests were performed using Prism 6.0c (Graphpad, San Diego, CA). $P < 0.05$ was considered a significant result.

PRIMARY HUMAN HEPATOCYTES

Cryopreserved human hepatocytes (BioreclamationIVT LLC, Waterbury, NY) were plated at 2×10^5 hepatocytes per well in tissue culture-treated 24-well polystyrene plates (Eppendorf, Hauppauge, NY) coated with rat tail type I collagen (50 μg/mL) patterned into microdomains as described.[30] The hepatocytes were cultured in Dulbecco Modified Eagle Media with high glucose, 10% fetal bovine serum (FBS), 1% insulin, transferrin, selenous acid premix (#354352; BD Biosciences, Bedford, MA), glucagon 7 ng/mL, dexamethasone 40 ng/mL, and 1% penicillin–streptomycin. Seeding of 3T3-J2 murine embryonic fibroblasts (9×10^4 cells in each well of a 24-well plate) occurred 12 hours after initial hepatocyte plating and was followed by replacement of hepatocyte culture medium and addition of ferric ammonium citrate (FAC; Sigma-Aldrich, St. Louis, MO) 24 hours after initial plating. At 24 or 48 hours after initial iron supplementation, cells were either fixed with 4% paraformaldehyde for 15 minutes or lysed for RNA extraction using the RNeasy kit (Qiagen). After washing the fixed cells with phosphate-buffered saline twice, the hepatocytes were stained with HCS Deep Red LipidTOX neutral lipid stain (Thermo Fisher, Waltham, MA), which was added to each well (1:500) for 30 minutes.

The hepatocytes were then imaged using a Nikon Eclipse Ti-E microscope.

ADENOVIRAL VECTORS

Adenoviral vectors containing *NNMT* complementary DNA or short hairpin RNA (shRNA) against *NNMT* were constructed previously as described[22] and purified by two rounds of cesium chloride centrifugation. Control viruses contained either green fluorescent protein or irrelevant shRNA. The titers of the purified viruses ranged from 5×10^{10} to 20×10^{10} plaque-forming units/mL.

PRIMARY MOUSE HEPATOCYTE ISOLATION, CULTURE, AND ADENOVIRUS KNOCKDOWN

Primary mouse hepatocytes were isolated from 8-week-old C57BL6 male mice by the collagenase perfusion method. Viable hepatocytes were enriched by Percoll gradient centrifugation. The hepatocytes were seeded on collagen-coated plates at a density of 300,000/mL in Williams' E medium/5% FBS. After a 4-hour attachment period, the medium was replaced with fresh Williams' E medium/5% FBS. Primary hepatocytes were infected by overnight exposure to adenovirus in Williams' E medium at a multiplicity of infection of 3 or 10. For *NNMT* knockdown, the hepatocytes were cultured for 96 hours to allow for the degradation of the endogenous protein. The medium was supplemented with FAC 0-150 μM 24 hours prior to the assessment of viability or extraction of RNA. Viability was assessed using 3-(4,5-dimethylthiazol 2-yl)-2,5-diphenyltetrazolium bromide as described.[31]

HUMAN SUBJECT RECRUITMENT

The human subject cohort comprised 53 morbidly obese subjects (9 men, 44 women) undergoing elective bariatric surgery at the Endocrinology Service of the Hospital Universitari de Girona Dr. Josep Trueta (Girona, Spain) as described.[22] All subjects gave written informed consent as part of a research protocol validated and approved by the ethical committee of the Hospital Universitari Dr. Josep Trueta (Comitè d'Ètica d'Investigació Clínica, approval number 2009046) in accordance with the ethical guidelines of the 1975 Declaration of Helsinki. Liver samples and sera were collected at the time of surgery. RNA was extracted, and serum iron, total iron binding capacity, and ferritin levels were determined as described in Supporting Methods.

Results

RNA SEQUENCING IDENTIFIED DIFFERENTIALLY REGULATED GENES IN HEPATIC IRON OVERLOAD

The *HJV*$^{-/-}$ mouse exhibits marked hepcidin deficiency that causes a severe iron-overload phenotype resembling the human disease juvenile hemochromatosis. While this provides a useful animal model for iron overload, we also wanted to use a model in which *hepcidin* transcripts increase in response to iron overload. To achieve this, C57BL6 mice were fed diets containing 2.5, 37.5, or 1,000 mg of iron per kilogram of food to produce iron deficiency, iron sufficiency, or iron overload, respectively (Fig. 1B). After 50 days, the mice were sacrificed and hepatic messenger RNA was extracted for next-generation sequencing while polar hepatic metabolites were isolated for analysis by LC-MS/MS. The RNA integrity number for each sample was >6. Assessments of read duplication, base call frequency, and read quality indicated excellent quality of the data.

As expected, hepatic iron levels rose with increasing iron content in the diet (1.4-fold for iron-sufficient versus iron-deficient diet and 3.1-fold for high-iron versus iron-deficient diet, n = 3 per group; $P = 0.001$ for high-iron diet versus iron-deficient diet) or in the *HJV*$^{-/-}$ cohort (18.5-fold for *HJV*$^{-/-}$ versus WT, n = 2 per group; $P = 0.006$) (Fig. 2A,D). Liver *hepcidin* transcript levels also increased with increasing dietary iron content (Fig. 2B) in the WT mice (8-fold for iron-sufficient versus iron-deficient diet and a further 2.6-fold for high-iron versus iron-sufficient diet; $P = 0.011$ for iron-sufficient versus iron-deficient diet and $P = 0.001$ for iron-sufficient versus high-iron diet). As expected, *hepcidin* expression was significantly reduced in the *HJV*$^{-/-}$ mice (Fig. 2E).

NNMT EXPRESSION DECREASED IN THE LIVERS OF BOTH NUTRITIONALLY AND GENETICALLY IRON OVERLOADED MICE

For the dietary iron-overload study, we used self-organizing maps to identify transcripts that expressed a

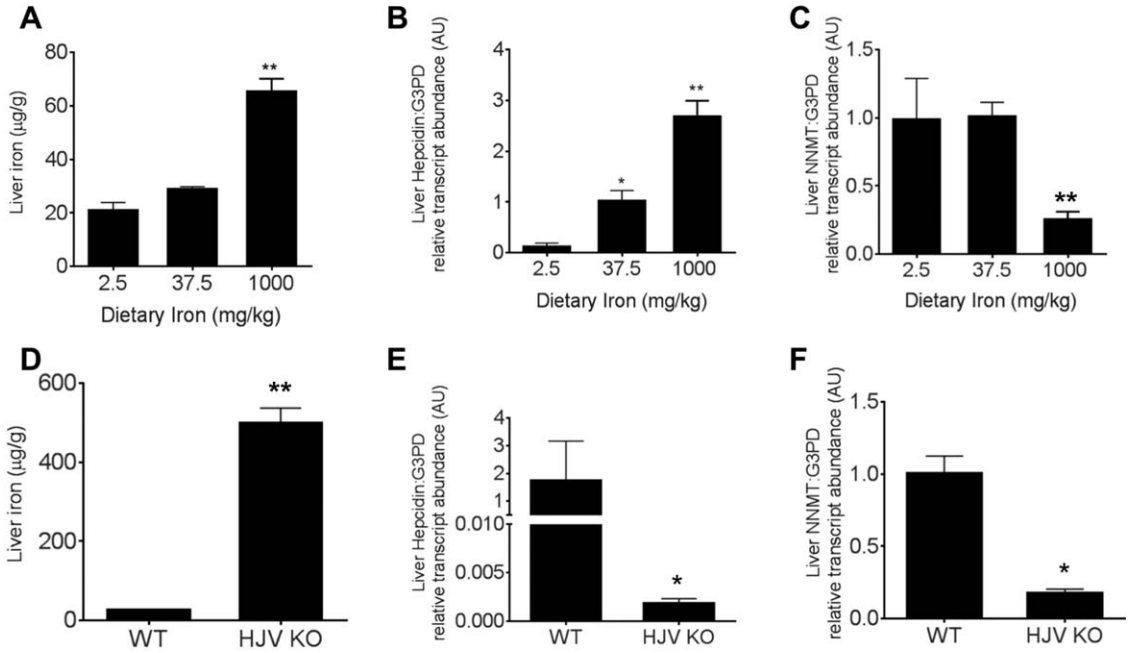

FIG. 2. Dietary and genetic models of iron overload exhibit increased hepatic iron stores and decreased *NNMT* expression. (A,D) Nonheme iron assays, (B,E) quantitative real-time reverse-transcription polymerase chain reaction analysis of *hepcidin*, and (C,F) *NNMT* transcript levels for the (A-C) dietary iron overload, (D-F) $HJV^{-/-}$ mice, and controls. *Hepcidin* and *NNMT* expression are reported as fold change over control mice with (B,C) an iron-sufficient diet (37.5 mg/kg) or (E,F) WT mice. Data shown are means +/− standard error measurements. * denotes $P < 0.05$ and ** denotes $P < 0.01$ by Student *t* test compared to the (A,B) low-iron group, (C) the iron-sufficient group, or (D-F) WT; n = 3 mice per group for (A-C) and 2 mice per group for (D-F). Abbreviations: G3PD, glyceraldehyde 3-phosphate dehydrogenase; KO, knockout.

strong association with increasing iron dose, while for the $HJV^{-/-}$ mice, we used FDR <0.05 and a mean fold change >2 to identify differentially regulated transcripts. We found 128 transcripts that were differentially regulated in the dietary iron study, while 688 transcripts were differentially regulated in the genetic model of iron overload. A total of 28 genes were differentially regulated in both the dietary and genetic iron-overload models. Of these genes, expression level changed in the same direction for 13 genes and in opposite directions for 15 genes (Table 1). Of the genes that were negatively regulated in both models, *NNMT* was the second most strongly suppressed in both the dietary and genetic iron-overload models. This effect appeared to be *hepcidin* independent as the dietary iron-overload model exhibits high *hepcidin* levels while the $HJV^{-/-}$ mice exhibit low *hepcidin* levels. We used quantitative real-time polymerase chain reaction to confirm the change in gene expression in both cohorts of mice. *NNMT* transcript levels decreased significantly in both the dietary and genetic models of iron overload (Fig. 2C,F). Using the DAVID 6.7 algorithm,[25,26] we found that two pathways were significantly altered in the genetic iron-overload model, peroxisome proliferator activated-receptor (PPAR) signaling and Huntington's disease genes (Table 2). The differentially regulated genes included genes involved in energy metabolism and apoptosis, including several NAM-dependent genes, e.g., *malic enzyme 1* (*ME1*) and *reduced NAD* [*NADH*]:*ubiquinone oxidoreductase* core subunits (*Ndufa2, Ndufa7, Ndufb7*, and *Ndufs7*).

ANALYSIS OF METABOLOMIC CHANGES CAUSED BY IRON OVERLOAD

The levels of polar metabolites extracted from the liver were compared between the dietary and genetic models of iron overload and their respective controls to identify the metabolites with absolute fold change >2 and *P* values ≤0.05 (Supporting Tables S2-S4). These metabolites were then grouped into pathways using Metaboanalyst 3.0 and ordered by *P* value. This analysis revealed that pathways involved in glucose and NAM metabolism were

TABLE 1. TRANSCRIPTS IDENTIFIED AS SIGNIFICANTLY ALTERED IN EXPRESSION IN BOTH DIETARY AND NUTRITIONAL IRON-OVERLOAD EXPERIMENTS

Gene	Dietary Iron Overload, SOM Vector	Genetic Iron Overload, Log_2 Fold Change	*Q* Value*	Direction†
Bhmt	−2.06	−1.41	0.0081	S
Nnmt	−2	−3.35	0.0022	S
Tfrc	−1.99	−2.89	0.0022	S
Mup21	−1.94	−1.12	0.0104	S
Hapln4	−1.93	−1.29	0.0469	S
Serpina12	−1.78	−4.69	0.0022	S
Cyp17a1	−1.56	−1.72	0.0022	S
Apoa4	−1.43	2.37	0.0022	S
Robo1	−1.33	−2.31	0.0022	S
Gbp6	−0.75	−1.55	0.0104	S
Kbtbd11	1.59	1.9	0.0442	S
Id3	1.84	2.08	0.0104	S
Bmp6	2.05	2.28	0.0104	S
Igfals	−2.19	1.62	0.0022	O
Syt3	−2.09	2	0.035	O
Extl1	−1.9	2.16	0.0022	O
Zap70	−1.8	1.39	0.0437	O
Serpinb8	−1.64	3.19	0.0022	O
Slco1a4	−1.51	1.25	0.0056	O
Slc10a2	−1.48	2.26	0.0022	O
Pdzk1ip1	1.28	−2.14	0.0337	O
Krt23	1.38	−2.26	0.0022	O
Fabp5	1.78	−1.86	0.0022	O
Gpr110	2.01	−1.45	0.0293	O
Hamp2 (HJV)	2.02	−4.23	0.0022	O
Vtcn1	2.02	3.55	0.0359	O
Lpl	2.04	−1.04	0.0355	O
Hamp (Hepcidin)	2.13	−6.41	0.0437	O

The change in transcription is expressed as an SOM vector relative to the WT animals and log_2 fold change relative to the low iron diet for the dietary iron overload and the genetic iron-overload models, respectively.
*Q value is the false discovery rate for the genetic iron-overload study.
†S represents transcripts that changed in the same direction; O represents transcripts that changed in opposite directions in the two models of iron overload.
Abbreviation: SOM, self-organizing map.

most significantly altered in the dietary iron-overload model (Fig. 3A) and were also highly significant in the genetic iron-overload model (Fig. 3B). Among the differentially regulated metabolites, NAM levels were increased in the livers of WT mice fed the high-iron diet compared to mice fed the low-iron diet (Fig. 3C).

EVALUATION OF NNMT TRANSCRIPT LEVELS IN HUMAN LIVERS

To determine if *NNMT* expression is associated with iron status in humans, we evaluated *NNMT* and *ferritin heavy chain* (*FTH*) transcript levels in liver biopsies obtained from 53 patients undergoing elective bariatric surgery and compared them to their serum iron indices. We found that *NNMT* transcript levels inversely correlated with measures of body iron stores (Fig. 4A-D), including serum ferritin ($P = 0.002$), percent transferrin saturation ($P = 0.02$), and *FTH* transcript levels ($P < 0.0001$), while there was an inverse trend with serum iron ($P = 0.06$). To validate whether iron loading suppresses *NNMT* transcript levels in human hepatocytes, we treated primary human hepatocytes with increasing doses of FAC and found a dose-dependent decrease in *NNMT* expression (Fig. 5A). Similar to our mouse models of iron overload, we observed decreased expression of *acyl-coenzyme A synthetase long-chain family members 3 and 5* (*ACSL3* and *ACSL5*) and fatty acid binding protein 4 (*FABP4*), all targets of PPAR-α signaling (Fig. 5A). Intriguingly, iron overload also increased lipid accumulation in the hepatocytes (Fig. 5B).

KNOCKDOWN OF NNMT EXACERBATES THE TOXICITY OF IRON OVERLOAD, WHILE NNMT OVEREXPRESSION IMPROVES HEPATOCYTE VIABILITY

To evaluate the effects of *NNMT* suppression on iron-induced toxicity, we infected primary mouse hepatocytes

TABLE 2. TRANSCRIPTS IN THE PPAR AND HUNTINGTON'S DISEASE SIGNALING PATHWAYS EXHIBIT LOWER LEVELS IN THE LIVERS OF *HJV*$^{-/-}$ MICE COMPARED TO WT MICE

Gene	Log_2 Fold Change *HJV*$^{-/-}$ vs WT	*Q* Value	Pathway
CD36	−0.74	5.0×10^{-5}	PPAR
ACSL3	−0.73	1.0×10^{-4}	PPAR
ACSL5	−0.80	1.0×10^{-4}	PPAR
Cyp4a12b	−0.42	5.0×10^{-5}	PPAR
DBI	−0.79	3.0×10^{-4}	PPAR
FABP2	−0.89	3.5×10^{-4}	PPAR
FABP4	−0.32	5.0×10^{-5}	PPAR
FABP5	−0.54	5.0×10^{-5}	PPAR
Lpl	−0.97	5.0×10^{-5}	PPAR
ME1	−0.63	1.0×10^{-4}	PPAR
Atp5d	1.83	4.0×10^{-4}	Huntington's
BBC3	2.76	7.5×10^{-4}	Huntington's
Bax	1.52	1.3×10^{-3}	Huntington's
Ndufa2	1.33	1.2×10^{-3}	Huntington's
Ndufa7	1.05	2.4×10^{-3}	Huntington's
Ndufb7	2.25	5.0×10^{-5}	Huntington's
Ndufs7	2.38	5.0×10^{-5}	Huntington's
Cox7a2l, Gm6969	1.95	2.0×10^{-4}	Huntington's
Polr2E	1.37	1.9×10^{-4}	Huntington's
Polr2F	1.85	1.2×10^{-3}	Huntington's
Gm8566, SOD1	3.48	3.4×10^{-3}	Huntington's
Uqcr11	2.56	4.0×10^{-4}	Huntington's
Uqcrq	1.97	7.5×10^{-4}	Huntington's

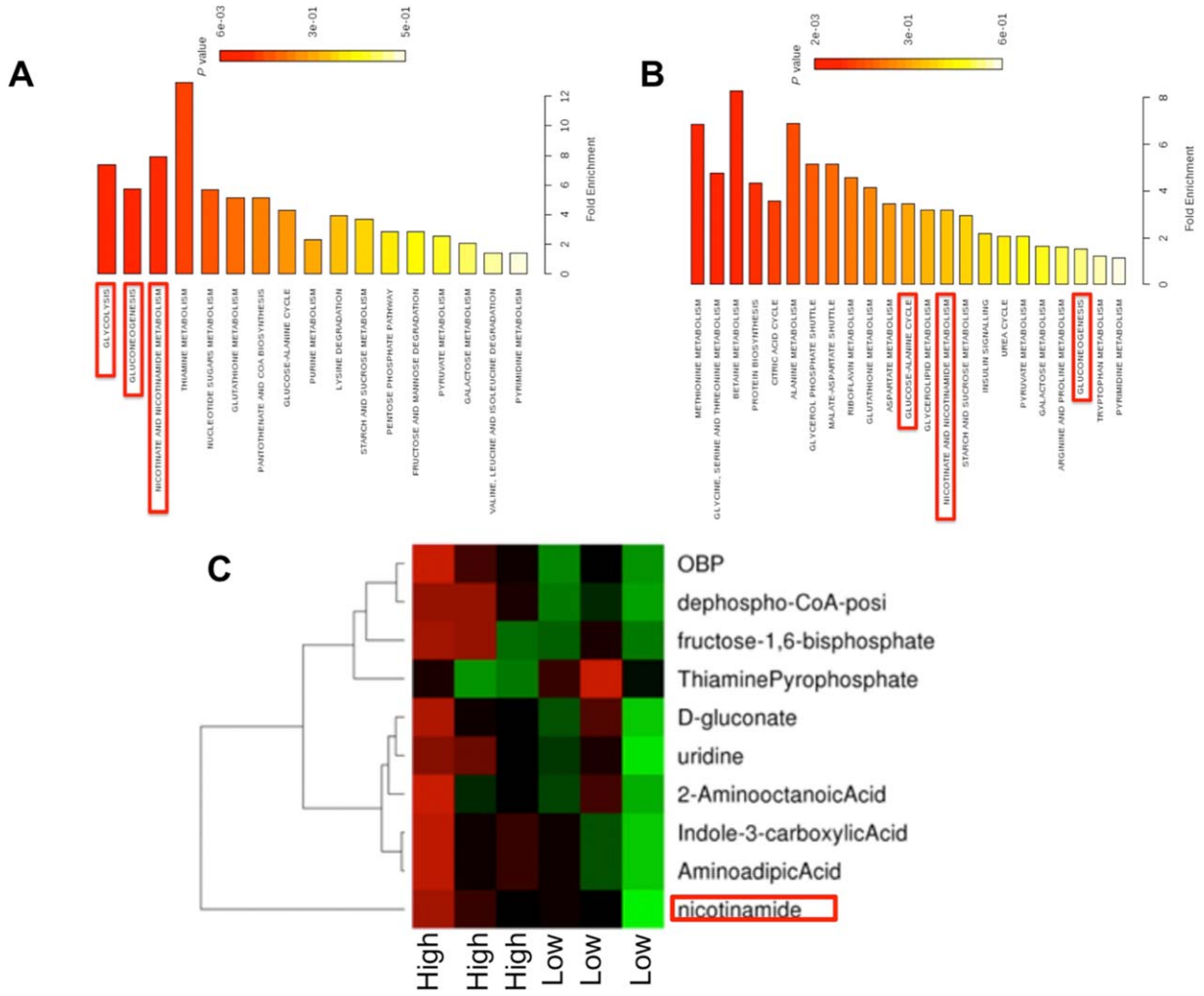

FIG. 3. Metabolites involved in glucose and NAM metabolism are differentially regulated in response to iron overload. (A,B) All significantly differentially regulated metabolites were grouped into pathways using Metaboanalyst 3.0 in the (A) dietary and (B) genetic iron-overload models and arranged from most significant (red) to least significant (yellow). (C) Heat map demonstrating a significant increase in NAM level in the dietary iron-overload model. Abbreviations: OBP, octulose-1,8-bisphosphate; CoA, coenzyme A.

with an adenoviral vector encoding shRNA targeting *NNMT* or a nontargeting control vector and treated the cells with FAC for 24 hours. We confirmed that the adenoviral vector targeting *NNMT* significantly decreased *NNMT* expression (Fig. 6A) while overexpression of NNMT increased NNMT transcript levels (Fig. 6B). Knockdown of *NNMT* enhanced iron-induced toxicity, as shown by decreased viability of iron-treated hepatocytes with *NNMT* knockdown compared to iron-treated controls infected with a nontargeting vector (Fig. 6C). In contrast, overexpression of *NNMT* increased primary mouse hepatocyte viability, even in the presence of iron overload (Fig. 6D). *NNMT* knockdown also significantly increased the iron-induced expression of *FTH* and markers of oxidative stress (*heme oxygenase 1* and *NAD(P)H quinone dehydrogenase 1*) and endoplasmic reticulum stress (*activating transcription factor 4*) (Fig. 6E). In contrast, overexpression of NNMT significantly reduced iron-induced expression of *FTH* and *activating transcription factor 4* (Fig. 6F).

Discussion

SYSTEMS BIOLOGY OF IRON OVERLOAD

Using two different models of hepatic iron overload, we identified a signature of 28 transcripts that are significantly altered in expression in the setting of

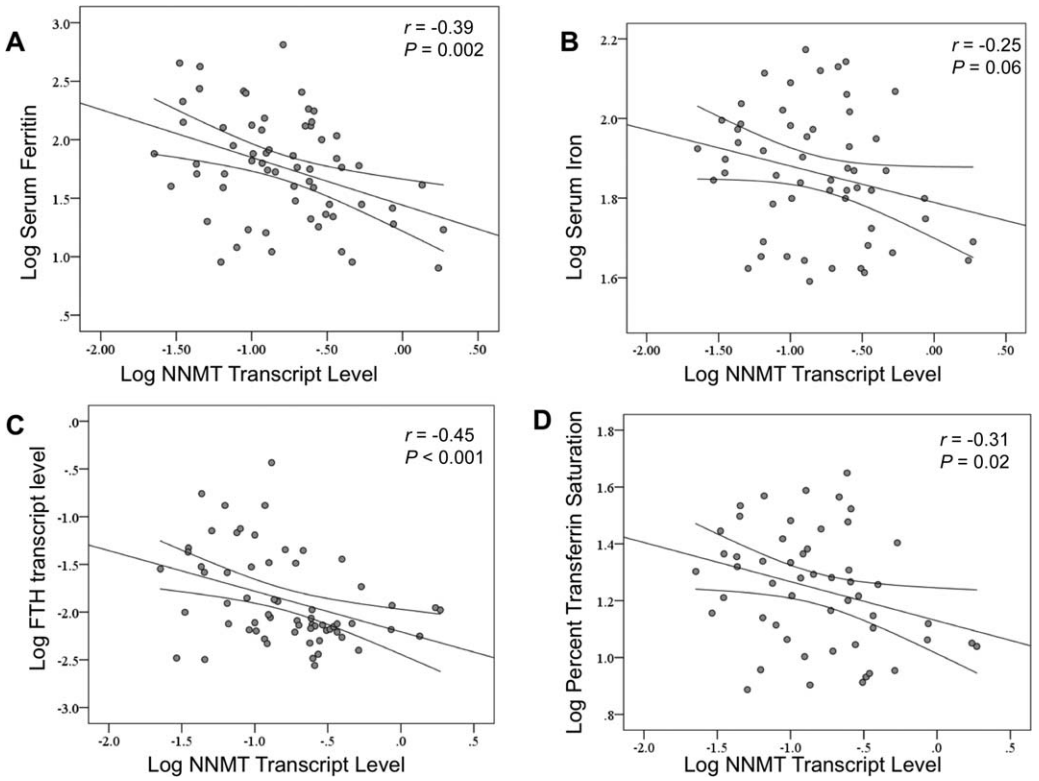

FIG. 4. NNMT transcript levels inversely correlate with measures of iron stores. Patients undergoing elective bariatric surgery provided liver biopsies and serum samples during their surgery to measure *NNMT* and *FTH* transcript levels and serum iron indices. Hepatic *NNMT* transcript levels inversely correlated with (A) serum ferritin level, (B) serum iron level, (C) hepatic *FTH* transcript level, (D) serum transferrin saturation; n = 53 patients.

iron overload. This signature includes several expected changes[32] in the transcriptional profile, including decreased *transferrin receptor* and increased *BMP6* and *Id3* (Table 1). Using the $HJV^{-/-}$ mice, which developed nearly 10-fold higher hepatic iron overload than the dietary model, we were able to identify two pathways that were significantly altered, Huntington's disease genes and PPAR signaling (Table 2). Several genes in both pathways regulate energy metabolism and require NAM derivatives for their function. *ME1*, an NADP-dependent enzyme, generates NADPH for fatty acid biosynthesis and decarboxylates malate, thus connecting the glycolytic and citric acid cycles.[33] *Ndufa2, Ndufa7, Ndufb7, Ndufs7* encode subunits of NADH:ubiquinone oxidoreductase, i.e., mitochondrial complex I, which transfers electrons from NADH to the respiratory chain.[34] Under conditions of oxidative stress, complex I dissociates from a larger mitochondrial supercomplex, which can result in increased production of reactive oxygen species by complex I.[34]

A recent transcriptional profile of the rat pancreas in the setting of iron overload demonstrated that one of the PPAR signaling targets, *Fabp2*, which we identified as down-regulated in our mouse model of iron overload, was significantly down-regulated in iron-overloaded rat pancreas.[35] FABPs are thought to play a role in the intracellular transport of long-chain fatty acids and their acyl-coenzyme A esters. Others have shown in mammalian models that iron overload leads to decreased hepatic PPAR-α expression,[36] decreased protein levels of PPAR-α targets,[37] and alterations in protein levels of enzymes involved in glucose metabolism and fatty acid oxidation.[38] Intriguingly, we observed decreased expression of PPAR signaling targets and increased lipid accumulation in iron-treated human hepatocytes (Fig. 5A,B). Conversely, others have demonstrated[39] that iron chelation reduces steatosis and increases PPAR-γ levels in the livers of *ob/ob* mice, a model of obesity and type 2 diabetes mellitus. Thus, it appears that iron overload may promote hepatic steatosis.

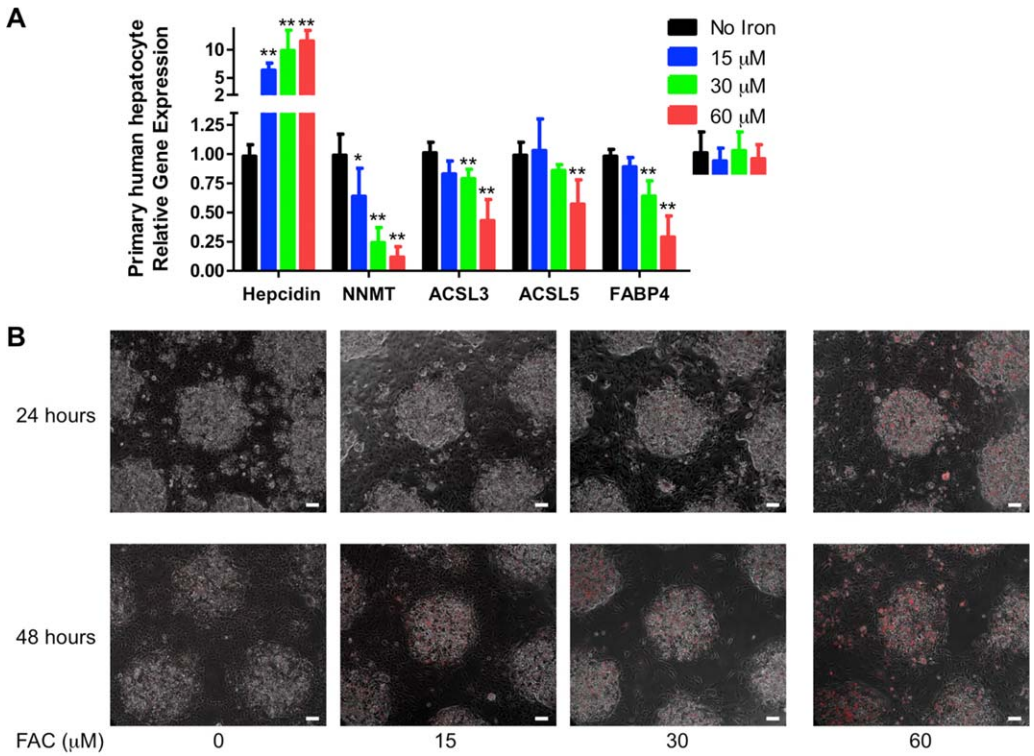

FIG. 5. The effect of iron loading on primary human hepatocytes. Primary human hepatocytes cultured with increasing doses of iron (FAC 0-60 μM) for (A,B) 24 hours or (B) 48 hours followed by harvesting RNA for quantitative real-time reverse-transcription polymerase chain reaction or fixation and staining for intracellular lipid accumulation with HCS Deep Red LipidTOX (Thermo Fisher). (A) Increasing doses of FAC were associated with decreased transcript levels of *NNMT* and PPAR-signaling targets *ACSL3, ACSL5*, and *FABP4*. * denotes $P < 0.05$, while ** denotes $P < 0.01$ compared to no iron control. (B) Treatment with increasing concentrations of iron was also associated with increased lipid staining in the hepatocytes on light microscopy. The scale bar denotes 100 μm.

We found that iron overload increased expression of a variety of pro-apoptotic genes implicated in Huntington's and other neurodegenerative diseases. Among the iron overload-induced genes was *Bax*, a pro-apoptotic protein that is regulated by nuclear factor kappa B and p53 signaling.[40] *Bax* is up-regulated in the cerebral cortex and striatum in the YAC128 mouse model of Huntington's disease.[41] In our models, iron overload also increased expression of *BCL binding component 3*, a pro-apoptotic protein that is involved in neurodegeneration.[42]

NNMT DEFICIENCY EXACERBATES THE TOXIC EFFECTS OF IRON OVERLOAD

Given the finding that iron overload altered the levels of transcripts and metabolites involved in energy and NAM metabolism, we were intrigued to study *NNMT* further. *NNMT* has gained attention as a potential drug target in cancer and obesity[21,22,43,44]; however, it has not been previously implicated in the pathophysiology of iron overload. We discovered that *NNMT* is a significantly repressed transcript in both the nutritional iron-overload model and the *HJV*$^{-/-}$ mouse. In our metabolomic analysis, dietary iron overload decreased hepatic *NNMT* transcript levels and increased hepatic NAM levels (Fig. 3C), which is consistent with decreased NNMT activity. We found that *NNMT* transcript levels negatively correlated with body iron stores in human patients (Fig. 4A-D), which indicates that this association of iron overload and *NNMT* suppression is likely to be conserved across species. Furthermore, we discovered that adenoviral knockdown of *NNMT* in mouse hepatocytes exacerbated cytotoxicity and enhanced expression of transcripts associated with oxidative damage and endoplasmic reticulum stress (Fig. 6C,E) while overexpression of NNMT partially reversed the toxic effects of iron overload (Fig. 6D,F). Because of the highly

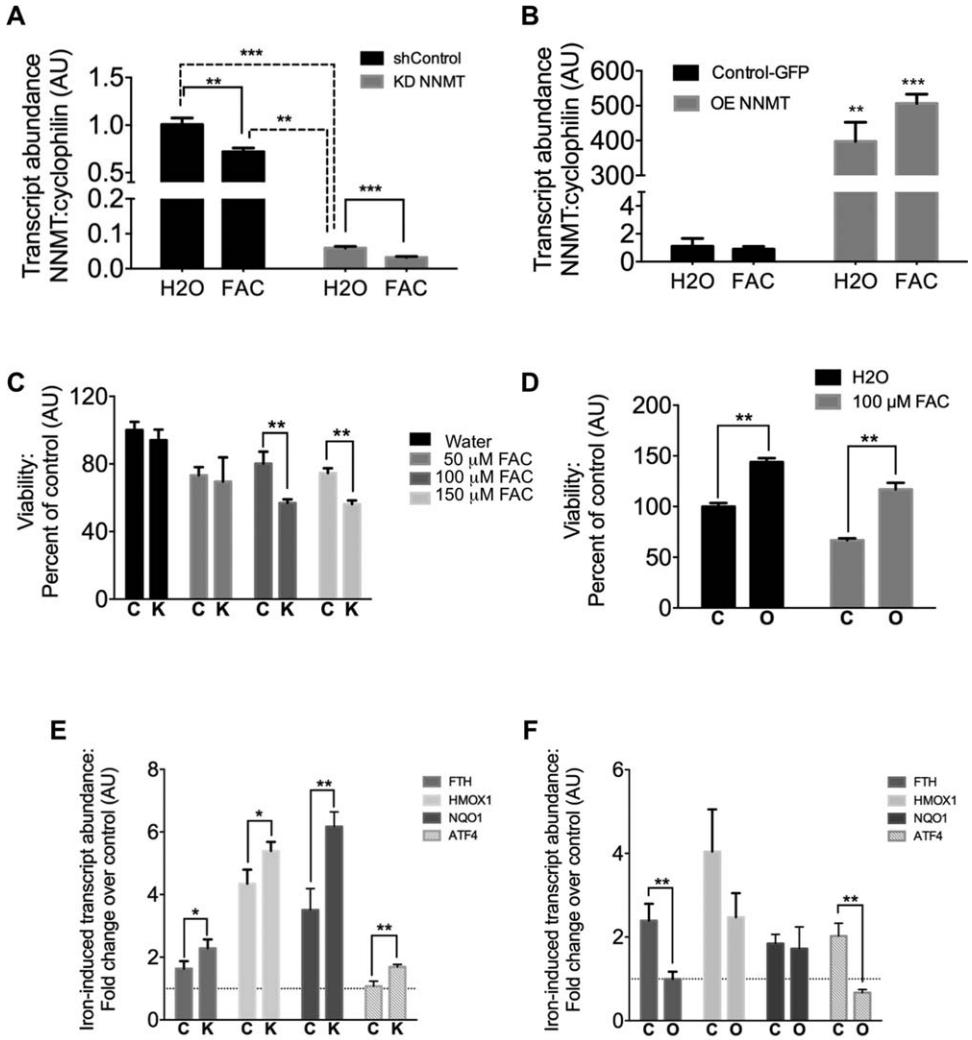

FIG. 6. *NNMT* knockdown exacerbates iron's hepatotoxicity, while overexpression improves viability. Primary mouse hepatocytes underwent (A,C,D) adenoviral knockdown of *NNMT* (K) or a nontargeting knockdown (C) or (B,D,F) overexpression of *NNMT* (O) or overexpression of *GFP* (C) followed by exposure for 24 hours to (A,E) FAC 30 μM, (C) 50-150 μM, (B,D,F) 100 μM, or (A,B,E,F) water and measurement of transcript levels by quantitative real-time reverse-transcription polymerase chain reaction or (C,D) viability by the MTT assay. *NNMT* knockdown decreased viability in the setting of iron treatment and increased expression of iron-induced transcripts related to oxidative and endoplasmic reticulum stress, while *NNMT* overexpression increased viability and decreased the expression of *FTH* and *ATF4*, which is a marker of endoplasmic reticulum stress. (E,F) Data shown are mean fold change in transcript abundance of iron-treated cells relative to control cells treated with water only, indicated by the dotted line. *, **, *** denote $P < 0.05$, $P < 0.01$, or $P < 0.001$ compared to controls, respectively, by Student t test; n = 3 biological replicates per group. Abbreviations: *ATF4, activating transcription factor 4;* GFP, green fluorescent protein; HMOX1, heme oxygenase 1; KD, knockdown; MTT, 3-(4,5-dimethylthiazol-2-yl)-2,5-diphenyltetrazolium bromide; NQO1, NAD(P)H quinone dehydrogenase 1; OE, overexpression.

variable NNMT expression in human livers (Fig. 4), we hypothesize that individuals with low *NNMT* expression may be predisposed to the adverse consequences of iron overload.

Whether genetic polymorphisms in *NNMT* increase the risk of liver and cardiovascular disease is an area of ongoing investigation. NNMT's action generates SAH, which is converted to homocysteine through SAH hydrolase.[45] Genetic variation in the *NNMT* locus has been linked to hyperhomocysteinemia,[45] a risk factor for cardiovascular disease. Over 200 single nucleotide polymorphisms have been identified, primarily in the noncoding regions of *NNMT*. One NNMT polymorphism in the noncoding region, rs694539, has been associated with hyperhomocysteinemia[46] and with nonalcoholic steatohepatitis,[47]

while another polymorphism in the coding region, rs1941404, is associated with hyperlipidemia.[48] The effect of these genetic polymorphisms on iron homeostasis has not yet been explored.

Mechanistically, NNMT regulates cellular metabolism by diverse pathways, including histone and protein methylation,[21,43] and stabilization of the NAD+-dependent deacetylase sirtuin 1 through generation of MNAM,[22] which serves as both a methyl and NAM sink.[49] In cancer cell lines cultured in physiological levels of methionine, *NNMT* knockdown increases SAM to SAH ratios, which increases protein methylation, while *NNMT* overexpression has the opposite effect.[43,44] *In vivo* models of *NNMT* deficiency have focused on the effects on glucose and lipid metabolism. Antisense knockdown of *NNMT* in mice that were fed a high-fat diet decreased the extent of obesity and increased methylation of histone H3 lysine 4 in white adipose tissue.[21] Liver-specific knockdown of *NNMT* in mice fed a high-fat diet increased serum and liver cholesterol levels, but the addition of *NNMT*'s product MNAM to the diet reversed these effects.[22]

In conclusion, we describe global changes in gene expression and metabolites in genetic and nutritional iron overload and implicate *NNMT* for the first time in the metabolic effect of iron. In future studies, we hope to identify the mechanisms by which down-regulation of *NNMT* exacerbates the toxic effects of iron overload and determine whether *NNMT* may be a drug target for iron-overload syndromes.

Acknowledgment: We thank Dr. Jon Asara, Mass Spectrometry Core, Beth Israel Deaconess Medical Center, for performing the metabolomic analysis.

REFERENCES

1) Ganz T, Nemeth E. Iron metabolism: interactions with normal and disordered erythropoiesis. Cold Spring Harb Perspect Med 2012;2:a011668.
2) Nemeth E, Tuttle MS, Powelson J, Vaughn MB, Donovan A, Ward DM, et al. Hepcidin regulates cellular iron efflux by binding to ferroportin and inducing its internalization. Science 2004; 306:2090-2093.
3) Wang RH, Li C, Xu X, Zheng Y, Xiao C, Zerfas P, et al. A role of SMAD4 in iron metabolism through the positive regulation of hepcidin expression. Cell Metab 2005;2:399-409.
4) Casanovas G, Mleczko-Sanecka K, Altamura S, Hentze MW, Muckenthaler MU. Bone morphogenetic protein (BMP)-responsive elements located in the proximal and distal hepcidin promoter are critical for its response to HJV/BMP/SMAD. J Mol Med (Berl) 2009;87:471-480.
5) Corradini E, Meynard D, Wu Q, Chen S, Ventura P, Pietrangelo A, et al. Serum and liver iron differently regulate the bone morphogenetic protein 6 (BMP6)-SMAD signaling pathway in mice. Hepatology 2011;54:273-284.
6) Babitt JL, Huang FW, Wrighting DM, Xia Y, Sidis Y, Samad TA, et al. Bone morphogenetic protein signaling by hemojuvelin regulates hepcidin expression. Nat Genet 2006;38:531-539.
7) Niederkofler V, Salie R, Arber S. Hemojuvelin is essential for dietary iron sensing, and its mutation leads to severe iron overload. J Clin Invest 2005;115:2180-2186.
8) Zhang AS, Anderson SA, Meyers KR, Hernandez C, Eisenstein RS, Enns CA. Evidence that inhibition of hemojuvelin shedding in response to iron is mediated through neogenin. J Biol Chem 2007;282:12547-12556.
9) Papanikolaou G, Tzilianos M, Christakis JI, Bogdanos D, Tsimirika K, MacFarlane J, et al. Hepcidin in iron overload disorders. Blood 2005;105:4103-4105.
10) Fernandez-Real JM, McClain D, Manco M. Mechanisms linking glucose homeostasis and iron metabolism toward the onset and progression of type 2 diabetes. Diabetes Care 2015;38:2169-2176.
11) Coimbra S, Catarino C, Santos-Silva A. The role of adipocytes in the modulation of iron metabolism in obesity. Obes Rev 2013;14:771-779.
12) Zimmermann MB, Zeder C, Muthayya S, Winichagoon P, Chaouki N, Aeberli I, et al. Adiposity in women and children from transition countries predicts decreased iron absorption, iron deficiency and a reduced response to iron fortification. Int J Obes (Lond) 2008;32:1098-1104.
13) Baumgartner J, Smuts CM, Aeberli I, Malan L, Tjalsma H, Zimmermann MB. Overweight impairs efficacy of iron supplementation in iron-deficient South African children: a randomized controlled intervention. Int J Obes (Lond) 2013;37:24-30.
14) Aeberli I, Hurrell RF, Zimmermann MB. Overweight children have higher circulating hepcidin concentrations and lower iron status but have dietary iron intakes and bioavailability comparable with normal weight children. Int J Obes (Lond) 2009;33:1111-1117.
15) Tussing-Humphreys LM, Nemeth E, Fantuzzi G, Freels S, Guzman G, Holterman AX, et al. Elevated systemic hepcidin and iron depletion in obese premenopausal females. Obesity (Silver Spring) 2010;18:1449-1456.
16) Yanoff LB, Menzie CM, Denkinger B, Sebring NG, McHugh T, Remaley AT, et al. Inflammation and iron deficiency in the hypoferremia of obesity. Int J Obes (Lond) 2007;31:1412-1419.
17) Salonen JT, Tuomainen TP, Nyyssonen K, Lakka HM, Punnonen K. Relation between iron stores and non-insulin dependent diabetes in men: case-control study. BMJ 1998;317: 727.
18) Bogan KL, Brenner C. Nicotinic acid, nicotinamide, and nicotinamide riboside: a molecular evaluation of NAD + precursor vitamins in human nutrition. Annu Rev Nutr 2008;28:115-130.
19) Cooper DL, Murrell DE, Roane DS, Harirforoosh S. Effects of formulation design on niacin therapeutics: mechanism of action, metabolism, and drug delivery. Int J Pharm 2015;490:55-64.
20) Trammell SA, Brenner C. NNMT: a bad actor in fat makes good in liver. Cell Metab 2015;22:200-201.
21) Kraus D, Yang Q, Kong D, Banks AS, Zhang L, Rodgers JT, et al. Nicotinamide N-methyltransferase knockdown protects against diet-induced obesity. Nature 2014;508:258-262.

22) Hong S, Moreno-Navarrete JM, Wei X, Kikukawa Y, Tzameli I, Prasad D, et al. Nicotinamide N-methyltransferase regulates hepatic nutrient metabolism through Sirt1 protein stabilization. Nat Med 2015;21:887-894.
23) Patchen B, Koppe T, Cheng A, Seo YA, Wessling-Resnick M, Fraenkel PG. Dietary supplementation with ipriflavone decreases hepatic iron stores in wild type mice. Blood Cells Mol Dis 2016; 60:36-43.
24) Nikkila J, Toronen P, Kaski S, Venna J, Castren E, Wong G. Analysis and visualization of gene expression data using self-organizing maps. Neural Netw 2002;15:953-966.
25) Huang da W, Sherman BT, Lempicki RA. Bioinformatics enrichment tools: paths toward the comprehensive functional analysis of large gene lists. Nucleic Acids Res 2009;37:1-13.
26) Huang da W, Sherman BT, Lempicki RA. Systematic and integrative analysis of large gene lists using DAVID bioinformatics resources. Nat Protoc 2009;4:44-57.
27) Smyth GK. Linear models and empirical bayes methods for assessing differential expression in microarray experiments. Stat Appl Genet Mol Biol 2004;3:Article3.
28) Xia J, Sinelnikov IV, Han B, Wishart DS. MetaboAnalyst 3.0-making metabolomics more meaningful. Nucleic Acids Res 2015; 43:W251-W257.
29) Zhen AW, Nguyen NH, Gibert Y, Motola S, Buckett P, Wessling-Resnick M, et al. The small molecule, genistein, increases hepcidin expression in human hepatocytes. Hepatology 2013;58:1315-1325.
30) Shlomai A, Schwartz RE, Ramanan V, Bhatta A, de Jong YP, Bhatia SN, et al. Modeling host interactions with hepatitis B virus using primary and induced pluripotent stem cell-derived hepatocellular systems. Proc Natl Acad Sci U S A 2014;111: 12193-12198.
31) Mosmann T. Rapid colorimetric assay for cellular growth and survival: application to proliferation and cytotoxicity assays. J Immunol Methods 1983;65:55-63.
32) Muckenthaler M, Roy CN, Custodio AO, Minana B, deGraaf J, Montross LK, et al. Regulatory defects in liver and intestine implicate abnormal hepcidin and Cybrd1 expression in mouse hemochromatosis. Nat Genet 2003;34:102-107.
33) Wen D, Liu D, Tang J, Dong L, Liu Y, Tao Z, et al. Malic enzyme 1 induces epithelial-mesenchymal transition and indicates poor prognosis in hepatocellular carcinoma. Tumour Biol 2015; 36:6211-6221.
34) Lenaz G, Tioli G, Falasca AI, Genova ML. Complex I function in mitochondrial supercomplexes. Biochim Biophys Acta 2016; 1857:991-1000.
35) Coffey R, Nam H, Knutson MD. Microarray analysis of rat pancreas reveals altered expression of Alox15 and regenerating islet-derived genes in response to iron deficiency and overload. PLoS One 2014;9:e86019.
36) Bonomo Lde F, Silva M, Oliveira Rde P, Silva ME, Pedrosa ML. Iron overload potentiates diet-induced hypercholesterolemia and reduces liver PPAR-alpha expression in hamsters. J Biochem Mol Toxicol 2012;26:224-229.
37) Petrak J, Myslivcova D, Halada P, Cmejla R, Cmejlova J, Vyoral D, et al. Iron-independent specific protein expression pattern in the liver of HFE-deficient mice. Int J Biochem Cell Biol 2007; 39:1006-1015.
38) Petrak J, Myslivcova D, Man P, Cmejla R, Cmejlova J, Vyoral D, et al. Proteomic analysis of hepatic iron overload in mice suggests dysregulation of urea cycle, impairment of fatty acid oxidation, and changes in the methylation cycle. Am J Physiol Gastrointest Liver Physiol 2007;292:G1490-G1498.
39) Xue H, Chen D, Zhong YK, Zhou ZD, Fang SX, Li MY, et al. Deferoxamine ameliorates hepatosteatosis via several mechanisms in ob/ob mice. Ann N Y Acad Sci 2016;1375:52-65.
40) Shou Y, Li N, Li L, Borowitz JL, Isom GE. NF-kappaB-mediated up-regulation of Bcl-X(S) and Bax contributes to cytochrome c release in cyanide-induced apoptosis. J Neurochem 2002;81:842-852.
41) Ehrnhoefer DE, Caron NS, Deng Y, Qiu X, Tsang M, Hayden MR. Laquinimod decreases Bax expression and reduces caspase-6 activation in neurons. Exp Neurol 2016;283:121-128.
42) Zhang Y, Shen K, Bai Y, Lv X, Huang R, Zhang W, et al. Mir143-BBC3 cascade reduces microglial survival via interplay between apoptosis and autophagy: implications for methamphetamine-mediated neurotoxicity. Autophagy 2016:12: 1538-1559.
43) Ulanovskaya OA, Zuhl AM, Cravatt BF. NNMT promotes epigenetic remodeling in cancer by creating a metabolic methylation sink. Nat Chem Biol 2013;9:300-306.
44) Shlomi T, Rabinowitz JD. Metabolism: cancer mistunes methylation. Nat Chem Biol 2013;9:293-294.
45) Souto JC, Blanco-Vaca F, Soria JM, Buil A, Almasy L, Ordonez-Llanos J, et al. A genomewide exploration suggests a new candidate gene at chromosome 11q23 as the major determinant of plasma homocysteine levels: results from the GAIT project. Am J Hum Genet 2005;76:925-933.
46) Zhang L, Miyaki K, Araki J, Nakayama T, Muramatsu M. The relation between nicotinamide N-methyltransferase gene polymorphism and plasma homocysteine concentration in healthy Japanese men. Thromb Res 2007;121:55-58.
47) Sazci A, Ozel MD, Ergul E, Aygun C. Association of nicotinamide-N-methyltransferase gene rs694539 variant with patients with nonalcoholic steatohepatitis. Genet Test Mol Biomarkers 2013;17:849-853.
48) Zhu XJ, Lin YJ, Chen W, Wang YH, Qiu LQ, Cai CX, et al. Physiological study on association between nicotinamide N-methyltransferase gene polymorphisms and hyperlipidemia. Biomed Res Int 2016;2016: 7521942.
49) Pissios P. Nicotinamide n-methyltransferase: more than a vitamin B3 clearance enzyme. Trends Endocrinol Metab 2017;28:340-353.

Supporting Information

Additional Supporting Information may be found at onlinelibrary.wiley.com/doi/10.1002/hep4.1083/full.